X-660-75-130
PREPRINT

NASA TM X- 70900

A REVIEW OF THE JOVIAN MAGNETOSPHERE BASED UPON PIONEER 10 AND 11

(NASA-TM-X-70900) A REVIEW OF THE JOVIAN MAGNETOSPHERE BASED UPON PIONEER 10 AND 11 (NASA) 45 p HC $3.75 CSCL 03B

N75-24643

Unclas
G3/91 23817

JAMES H. TRAINOR

MAY 1975

GODDARD SPACE FLIGHT CENTER
GREENBELT, MARYLAND

A REVIEW OF THE JOVIAN MAGNETOSPHERE

BASED UPON PIONEER 10 AND 11

James H. Trainor

Laboratory for High Energy Astrophysics
NASA/Goddard Space Flight Center
Greenbelt, Maryland 20771

Prepared for: The Annual Review Session
18th Annual COSPAR Meeting
June 3, 1975
Varna, Bulgaria

COSPAR Paper R.2.1

A REVIEW OF THE JOVIAN MAGNETOSPHERE BASED UPON PIONEER 10 AND 11

James H. Trainor

Laboratory for High Energy Astrophysics
NASA/Goddard Space Flight Center
Greenbelt, Maryland 20771
United States of America

ABSTRACT.

This paper reviews the data derived from the plasma, magnetic field and energetic particle experiments on the Pioneer 10 and 11 spacecraft which encountered Jupiter in December of 1973 and 1974, respectively. The major features and phenomena are surveyed with the goal of leading to a consistent picture or model of this giant magnetosphere which is so different from that of our own earth.

1. Introduction.

The Pioneer 10 and 11 encounters with Jupiter have been two of the most exciting occurrences in the past 18 months. Jupiter has long held the promise of great excitement - scientific and otherwise - and this has been especially true for scientists interested in the magnetosphere. For many years it has been clear that Jupiter had a substantial magnetic field, and that contained in this magnetic field within a few Jupiter radii (R_J) of the surface were large fluxes of energetic electrons with energies extending to tens of MeV [1, 2].

The decimetric radio emission from Jupiter was interpreted as synchrotron emission by these electrons spiraling in the strong magnetic field, but the level of the emission was such that we received no information on the extent of the electron belt beyond $\sim$10 R_J. Based upon our knowledge of the earth's magnetosphere, we expected a large magnetosphere preceded by a detached bow shock on the solar side of Jupiter. In the late 1960's, many estimates of the location of the bow shock placed it at $\sim$100 R_J at the subsolar point. These estimates were based upon predictions or assumptions concerning the solar wind, the Jovian magnetic field and upon analogy with the earth's magnetosphere. Several of these assumptions turned out to be wrong in detail, but Pioneer indeed found a bow shock at $\sim$100 R_J near the noon meridian under normal solar wind conditions [3, 4].

Predictions of the position of the magnetopause were more variable, most being in the range 50 to 75 R_J; and, indeed, Jupiter has shown us multiple locations of the magnetopause ranging from 46.5 R_j to 97.3 R_j again within 40° of the subsolar point. The Jovian magnetosphere and many of the dominant mechanisms at work there turn out to be significantly different from those of the earth. In making that statement I must point out that there is much we don't know concerning the Jovian magnetosphere and probably won't know until long-lived Jovian orbiters are a reality. The dusk quadrant and tail region of the magnetosphere are completely unexplored.

Nevertheless, it is clear that our predictions about the Jovian magnetic field, the trapped nuclear particles and the plasma within the magnetosphere were wrong in many regions of the magnetosphere. We predicted a field larger than found, predicted smaller fluxes of energetic electrons than found, and no one predicted the detailed complex plasma conditions found within the magnetospheres; and the plasma turns out to be a dominant factor in the topology of the magnetosphere.

It is my purpose in the limited time and space available to demonstrate the essential features of the Jovian magnetosphere as learned from the recent encounter of Pioneer 10 and 11 with Jupiter.

2. The Pioneer 10 and 11 Missions.

Figure 1 is a sketch of the Pioneer spacecraft showing its salient features [5]. Physically, the design is dominated by the parabolic dish for the S-band communications system, the long boom for the helium vector magnetometer and the shorter booms holding the radioisotope thermoelectric power supplies. Pioneer 11 also had a high-field flux gate magnetometer in case of very large fields close to Jupiter. Four energetic particle experiments were positioned around and in the rear compartment so they received a scan view with spacecraft spin. These experiments included cosmic radiation sensors as well as trapped radiation sensors. A plasma analyzer mounted behind the communications dish views through it towards the solar direction. This instrument was designed primarily for solar wind measurements in interplanetary space, but was especially important in giving some good information regarding the distribution and role of the plasma within the magnetosphere.

Table 1 lists the concerned science instruments on Pioneer 10 and 11, the principal investigator and his institution. These instruments comprise an extremely lightweight, low power and complex set of instruments designed to work in a high radiation environment. It is not possible to describe them and their operation in this paper, but such descriptions have already been published [6, 7, 8, 9, 10, 11, 12]. Many salient features of their operation will be apparent from a discussion of the results.

An understanding of the Pioneer 10 and 11 trajectories approaching and through the Jovian magnetosphere is necessary for understanding the data.

Figure 2 summarizes these trajectories in a Jupiter frame of reference [5]. The left picture shows the trajectories projected on a plane parallel to the ecliptic while that on the right shows the view as seen from earth. Pioneer 10 followed a prograde trajectory inclined about 14° to the Jovian equator, while Pioneer 11 followed a retrograde trajectory inclined at about 50°. Pioneer 10 spent most of its time within the magnetosphere fairly near the magnetic equator, while Pioneer 11 spent most of its time in the inner magnetosphere at latitudes greater than 40° with the exception of ∿2 hours around periapsis.

Both spacecraft approached Jupiter from the morning quadrant with Pioneer 10 being only about 30° from the sun line. The exit trajectories are quite different, however, with Pioneer 10 exiting at ∿110° on the dawn side while Pioneer 11 left Jupiter at high latitudes towards the solar direction. From an azimuthal point-of-view, Pioneer 10 inbound and Pioneer 11 outbound sampled similar subsolar regions of the magnetosphere, while Pioneer 10 outbound traversed the dawn region and Pioneer 11 inbound was intermediate. The Pioneer 11 trajectory gave much better latitude and longitude coverage, as well as going closer to the planet - inside 1.6 R_J vs. 2.8 R_J for Pioneer 10. Note that these trajectories really did not allow observation of the dusk side or the tail region of the magnetosphere at all.

3. The Jovian Plasma.

The plasma analyzer allows clear identification of the bow shock crossings (Figure 3), the magnetosheath region and the magnetopause [3, 4, 14]. These data are summarized in Figure 4, where the bow shock and magnetopause crossing data are shown rotated on to a common plane parallel to the ecliptic and viewed from the north. Multiple observations of the bow shock and magnetopause are explained as a result of the motion of these surfaces in response to changing solar wind pressures [8]. These observations are consistent with the magnetic field and energetic particle measurements in describing the outer magnetosphere as a highly variable "spongy region" - a region easily and apparently often compressed up to a factor of two.

From Figure 4 we can see that Pioneer 11 remained within the magnetosphere on its outbound trajectory until $\sim 80\ R_J$ at a location $\sim 30°$ northward from the nose. This is clearly evidence for a fairly thick, blunt magnetosphere in contrast to the model of a disk-like magnetosphere based largely on the energetic particle results from Pioneer 10 [6, 9, 10, 11, 12]. I will return to the topic several times in this review, but it is quite clear that there are large spatial variations occurring in Jupiter's magnetosphere; and apparently there are large azimuthal and/or time variations in the outer portions of the magnetosphere.

The plasma analyzer on Pioneer 10 and 11 was designed for detailed measurement of the solar wind and planetary magnetosheath. Consequently, it lacks the sensitivity and energy range required for thorough investigations of the hot plasma found within a magnetosphere. A special instrument was not included in the instrument complement on Pioneer, apparently because of the severe competition for the available weight (30 Kg) and power (24 watts). Nevertheless, the instrument had just enough sensitivity at many times, and even though the investigators also had special problems in removing the substantial background currents due to penetrating energetic charged particles, the end result is that this investigation has now provided direct evidence of several remarkable plasma domains within the Jovian magnetosphere [13].

Figure 5 summarizes many of the measurements. The density of protons in the energy range 108 eV to 4.80 KeV is plotted vs. time and L value in R_j; and the L region traversed by the moons Europa, Io and Amalthea are noted. It is apparent that inside the orbit of Io, there is a huge plasma sphere which extended at least to perijove at 2.8 R_j. The protons in this plasma have characteristic thermal energies of ∿100 eV. The authors note that the flux tubes through which Io passes are positioned on the plasmapause and that the relationship of Io to this plasmapause is quite likely to be fundamental to the Io-modulation of decametric radio emissions [13].

The measurements and analysis are not limited to the region just discussed. Figure 6 gives an overview of the region out to 25 R_j. Beyond the plasmapause, a great torus of plasma, or ring current, is found encircling Jupiter in the region L ∿ 8 R_j to ∿12 R_j. Densities are ∿10-15 protons cm^{-3} and typical thermal energies are ∿400 eV. The energy density in the plasma is high enough to significantly distort the magnetic field. From the measurements during inbound and outbound traversals, it is reported that this plasma torus or ring current is approximately axially symmetric. The moon Europa is completely immersed in the ring current, but there is no indication of interactive effects as with Io. At larger distances, this ring current extends into a thin plasma disk as had already been inferred from the magnetic field measurements [6]. Finally, and importantly, the authors conclude that the source of these protons is the Jovian ionosphere, basing the conclusion largely on the lack of any known sensible mechanism for transporting solar wind ions from the magnetopause to these locations deep in the magnetosphere, and which could account for the high densities and low energies observed.

4. Jovian Magnetic Field.

The Pioneer 10 encounter provided a good picture of the Jovian magnetic field [6, 15]. The data from the inbound trajectory is summarized in Figures 7 and 8, along with the projected dipole field behavior. From these hourly averages, it is apparent that the far field is inflated and contains a fairly high degree of disorder, especially as seen in the direction of the field. After crossing the magnetopause, the field remains essentially constant to ∿55 R_J. the field strength near the 98 R_J magnetopause crossing was larger by an order of magnitude than the projected dipole field. Inside the magnetopause there is a strong tendency of the field to point southward until about 80 R_J and then a trend for the direction to move towards the equator. In this region there are not apparent features in the amplitude and phase of the field which one would expect from a rotating, offset and tilted dipole. Inside 40 R_J, however, the angle δ clearly shows these associated variations. It appeared that a magnetic field - highly inflated by plasma - was being observed. On Day 335, when Pioneer 10 was at $\sim$50 R_J, the magnetosphere was compressed to a dimension inside Pioneer 10; suddenly for several hours, Pioneer 10 was in the magnetosheath again [3, 14]. This is further evidence of a "soft" outer magnetosphere. And finally, in agreement with the plasma analyzer analysis, the detailed magnetometer measurements clearly show passage through a current sheet, similar to that found in the earth's magnetotail. This intense current sheet gives rise to fields that are much larger than the dipole field and lying parallel to the Jovigraphic equatorial plane.

Similar data acquired during the outbound trajectory of Pioneer 10 are shown in Figures 9 and 10, and one easily notes that the field character is quite different here near the dawn meridian. The periodic changes in field direction due to rotation of the offset dipole are visible with the expected amplitude only to $\sim$20 R_J, however; and by the time 30 R_J has been reached, the average field is nearly parallel to the Jovigraphic equator. This behavior persists all the way to the magnetopause.

Inside 20 R_J, the field became increasingly dipolar in character, and the Pioneer 10 data inside $\sim$7 R_J converges well to a dipole of moment 4.0 Gauss R_J^3, and a tilt angle of 11° (at a System III longitude of 222°) with respect to Jupiter rotation axis and the dipole is displaced $\sim$0.11 R_J from the center of Jupiter [6].

Figure 11 summarizes the conclusions drawn from all the data. The large outward extension of the field beyond 40 R_J requires an outward force whose only realistic origin is the centrifugal force on a plasma corotating with the field. The current sheet is parallel to Jupiter's equator in the outer magnetosphere and does not lie in the magnetic equator except near the planet [6].

I have discussed the trajectory of Pioneer 10 briefly before. The trajectory was prograde, and near the planet a relatively limited range of longitudes and latitudes were directly sampled. The trajectory of Pioneer 11 was retrograde, and when inside 7 R_J for 11 hours, covered 660° in longitude from $\lambda_{III} = 30°$ to $\lambda_{III} = 330°$, and latitudes from -30° to +50° while passing within 0.6 R_J of the planet's surface. One expects, therefore, to get a better sampling and measurement. Measurements of the helium vector magnetometer showed 5 percent discrepancy with the Pioneer 10 model - dipole moment of 4.225 G R_J^3, tilt angle of 10.77° and System III longitude of 230.9° [15]. They also have presented the results of a spherical harmonic analysis consisting of interior dipole, quadrapole and octapole, and an exterior dipole and quadrapole. The fit appears to be good, and this representation has been used to derive contours of magnetic field strength at the surface of Jupiter, as seen in Figure 12. The maximum field strengths at the north and south poles are 14 and 11 gauss, respectively.

Pioneer 11 also included a high-field flux gate magnetometer [7] which had been included on the chance that the Jovian field close to the planet might be so large as to exceed the range of the helium vector magnetometer. In a spherical harmonic representation, this experiment measured a dipole term of 4.02 gauss

R_J^3 at a tilt angle of 9.0° and a System II longitude of 229°. However, the quadrapole and octapole moments are very large, being 50% and 90%, respectively, of the dipole moment. This leads to significant and complex deviations from a dipole topology inside 4 R_J and is in detailed variance with the results of the helium vector magnetometer measurements.

For comparison, the deduced Jovian surface field and field at 2 R_J are shown in Figure 13. While there are similarities to Figure 12, there are substantial differences. The north polar field is 22 gauss vs. 14 gauss, for instance. The convolutions in the field are more pronounced. One notes also that the foot of the field through Io is localized to longitudes of 75° to 215° in System III, and its path is not what one might expect. The magnitudes of these higher-order moments is such that considerable L shell splitting is expected [7].

The authors have also calculated the , values expected from this O_3 model along the Pioneer 11 trajectory for the particular case of 90° pitch angle particles, and this is shown in Figure 14. Also shown are the corresponding data points for the D_2 model [6] derived from Pioneer 10 and a dipole model [10] derived from energetic particle data, as well as the L regions covered by Io and Amalthea, based on the O_3 model. Large differences are apparent; and it should be possible for energetic particle experiments to add further information, since Io and Amalthea do remove trapped particles from the radiation belts, and one could see, for instance, from the inbound Amalthea crossing that substantially different times of crossing are predicted by the different models.

5. Energetic Particles.

From the particle point of view, the magnetosphere of Jupiter is very exciting and also it is still more than just a little confusing. One also must keep in mind that we have sampled only a limited region of the magnetosphere; and there we've found large temporal, latitudinal and azimuthal variations at times. We have had no glimpse of the afternoon quadrant or the night hemisphere except quite near the planet. We know nothing of the magnetotail, a region most important in the case of the earth's magnetosphere.

It is clear, however, that Jupiter's magnetosphere is quite different from that of the earth in many respects [9, 10, 12, 17, 18, 19, 20, 21]. Approaching the bow shock fluxes of protons with energies to several MeV are commonly seen, while Pioneer 10 and 11 instruments observed energetic electrons from Jupiter while up to 2 A.U. away. Indeed, we now know that we've been observing these Jovian electrons at earth orbit - they were previously referred to as quiet time electron increases [16]. The magnetopause, however, is a sharp boundary for confinement of energetic particles independent of their radial position; although its location is variable to a factor of 2 apparently as a result of changes in solar wind pressure. The outer Jovian magnetosphere is a region extending in to 40 or 50 R_J, a region of quasi-trapping and diffusion, while the region inside $\sim$25 R_J is apparently the really stable trapping region. In the intermediate region from ~50 R_j to ~25 R_j, planetary rotation effects, particle acceleration and particle injection become apparent. I will now proceed to demonstrate these and other phenomena with data from the Pioneer particle instruments.

Figure 15 shows an overview of the Pioneer 11 encounter for low energy protons and high energy electrons [17]. Clearly seen are the particles leaking from the magnetosphere, the multiple boundary crossings, the appearance of strong 10-hour periodicities within ~50 R_j, approximately constant peak fluxes at low latitudes from near the magnetopause to ~25 R_j, and central core region of intense particle fluxes.

Figure 16 shows electron spectral data from Pioneer 10 [21]. This is typical, showing hard power law spectra over the entire region outside ~25 R_j. The spectra are actually somewhat harder in the outermost regions and are quite similar to the spectra of electrons observed leaking from Jupiter. Proton energy spectra in the energy region 100 KeV to 20 MeV commonly show a power law spectrum with exponent varying from -4 in the outermost regions to -3 near the planet. On Pioneer 10 the spectra inside ~40 R_j are not well fitted by power law spectra [21].

The angular distribution of the electrons and protons offer good insight to the processes occurring. Figure 17 demonstrates rather typical behavior for electrons and protons in the Jovian magnetospheres [21]. The electrons almost always demonstrate a nearly isotropic distribution while the protons clearly show a corotation anisotropy, other anisotropies probably due to acceleration and also the rocking motion of the magnetosphere associated with the planetary rotation.

Some of the results of a harmonic analysis of the proton angular distribution are shown in Figure 18 [21], where the relative amplitude and phase of the first harmonic of the 1.2 to 2.1 MeV protons are shown as Pioneer 10 traverses the region from $\sim 50 R_j$ inwards. The dashed line on the A_1/A_o plot represents the magnitude of the effect expected from corotation alone for a spectrum going as E^{-4}, for instance. Examination of the θ_1 plot shows that there are large systematic fluctuations that steadily decrease and that at $\sim 23\ R_j$ there is a well-defined "hinge joint," the particle coming from $\theta_1 = 90°$, as expected from corotation. Inside this point there would appear to be rigid rotation of the field with the rotation of the planet.

Going to the A_1/A_o plot, agreement with the innermost values of A_1/A_o is pretty good; however, the larger peaks in A_1/A_o between 25 and 50 R_j were not understood at first. The minima are apparently a clear indication that rigid corotation doesn't exist at that point. It was only after correlation with detailed magnetic field data [6] that the explanation of the peaks in A_1/A_o became obvious. These large anisotropies occurred at high latitudes, at reduced fluxes and their direction is along the field line. It is apparent that we are seeing particle injection and perhaps acceleration, and the effect is emphasized in the data at the higher latitudes because of the lower overall trapped fluxes. These particular fluxes are traveling along the field line into the atmosphere and are not associated with corotation at all. Since the field lines are apparently closed on the sunlit side of the of the magnetosphere, it may well be that these protons are being injected and accelerated from the ionosphere at the other end of the field line, or perhaps they are flowing down the field lines in the equatorial current sheet from the inner region where the dominant particle acceleration takes place.

These particles also give us insight into the deformation of the magnetosphere. Previous data had demonstrated the strong 10-hour periodicity in particle fluxes associated with the position of the Jovimagnetic equator as it moves with respect to Pioneer at the planetary rotation rate. The times of minima are clearest to note, and Fillius and McIlwain have plotted the System III longitude of occurrence of the minima in the >6 MeV electron fluxes on a polar plot shown in Figure 19 for both inbound and outbound Pioneer 10 trajectories [12]. The arrow marks the direction of the tilt of the internal dipole field, where one expects the minima to line up in the absence of external currents.

Inside 20 R_J, the minima and therefore the equator was found where it was expected to be. Outbound there are clear indications for the minima to lag their expected locations in the sense of the "garden hose" direction - e.g., it appears that the outer magnetosphere is lagging the rigid corotation of the inner magnetosphere. On the sunward side of the magnetosphere the alignment is good inside 25 R_J, but beyond 50 R_J it either leads by 90° or lags by 270°. This is obviously quite different from the dawn side and is unexplained really. The problem is complicated by the fact that while near 50 R_J inbound, the magnetosphere was compressed such that Pioneer 10 found itself suddenly in the magnetosheath for many hours, and this occurrence may have markedly disturbed the condition and mechanisms at work.

In order to understand the effects measured in the inner core region of the magnetosphere, the "wiggle diagrams" shown in Figure 20 are most useful [22]. In this inner region of the magnetosphere, the Pioneer 10 and Pioneer 11 measurements are directly comparable only at two points, both near L (magnetic shell parameter) = 12. From ∿2000 on 2 December to ∿0130 on 3 December, Pioneer 11 was on L shells ∿12 R_J while moving from 13° to 44° south magnetic latitude. Then, while remaining at essentially constant magnetic latitude, Pioneer 11 traversed L shells down to L = 3.4 at ∿0445 when it passed through -40° magnetic latitude on its way to the equator 1 hour later, and exited Jupiter moving towards the sun and to high latitudes.

In Figure 21 the count rate corresponding to electrons with energy greater than 21 MeV [10] are shown plotted vs. L, wherein the left of the figure L has been calculated based upon the D_2 model of Smith <u>et al</u>. [6] from Pioneer 10. It is apparent that the D_2 model was insufficient to rectify these and other similar results. The right side of Figure 21 shows similar data plotted against a field model with a 9.5° tilt which produced coincident inbound and outbound data, except for a small loop at the smallest L values. This loop was minimized by allowing the power m of the pitch angle dependence to be a function of L as noted [10]. The Pioneer 11 magnetic field results are much closer to this model derived from the particles. When the data are plotted against L derived from the particle model, one expects and gets the iso-counting rate contours shown in Figure 22 [10]. The correspondence between the data of Pioneer 10 and 11 is good in this inner region.

Large fluxes of penetrating protons are found only in the inner region of the magnetosphere of Jupiter. Figure 23 shows protons fluxes measured in two energy groups on Pioneer 11 [19]. At beginning times on this plot, the 1.2 to 2.1 MeV protons were recovering from a minimum flux associated with the planet rotation, but the flux of 14.8 to 21.2 MeV protons had never really been appreciable outside 15 R_J. Up until ∿0300, the fluxes behaved in a fashion to be expected from the trajectory presented in Figure 20. While sampling L shells crossed by the orbit of Io, decreases of ∿3.6 in the fluxes of 14.8 to 21.2 MeV protons were noted, similar to the effects seen on Pioneer 10. A huge effect is seen for the low-energy protons. Io is effective in removing more than 99% of the protons in this energy interval. This factor of ∿100 decrease compares with a factor of ∿60 at much lower latitudes, and the larger effect there is in agreement with predictions [23].

Small effects are seen crossing Amalthea's orbit, but a major feature is noted just after perijove, where a large sharp peak in the high-energy protons occurs. The peak shown for the low-energy protons is false, being the result of saturation of the low-level anticoincidence rates in this sensor. Even the 14.8 to 21.2 MeV fluxes shown here have had to be corrected, and the true peak fluxes including alpha particles could be a factor of 2 or 3 higher than the estimated peak value of $\sim 4 \times 10^6$ protons $cm^{-2} sec^{-1}$. This feature was unexpected, but explanations are progressing as we shall see. Outbound, the spacecraft moved very rapidly to high latitudes, exiting the intense radiation belts abruptly.

The same 1.2 to 2.1 MeV data is shown on an expanded scale in Figure 24 together with angular distributions measured on the spacecraft and the projection of the magnetic field vector on the sector plane [19]. These data, together with the calculations (O_3 model) from the Pioneer 11 magnetid field data [7], lead to considerably more insight into these magnetospheric phenomena. Outside L $\sim$10 R_J, the O_3 model calculations [24] show that the loss cone was less than 5° and increased rapidly up to $\sim$30° as Pioneer 11 came across the region swept by Io, decreasing to small values again as Pioneer 11 moved in towards the equator. A somewhat similar effect occurred outbound. It seems quite clear that, as the counting rate levels off before reaching Io, we are observing the progressive loss of protons into the atmosphere due to the growing loss cone. The effect is even more pronounced at the count rate minimum inside Io. As Pioneer 11 moved inward further, the loss cone rapidly shrank, the fluxes rapidly increased and the angular distribution moved towards a more isotropic distribution.

Figure 25 shows other data inside 10 R_J [17]. I'm particularly interested in the fission cell count rates inside 2 R_J

outbound and the response of the ECD detector plotted just at the top of the figure. The fission cell is normally responding to protons (E_p > 35 MeV); but in this instance, this count rate would correspond to a peak proton flux of $\sim 1.3 \times 10^8$ $cm^{-2}sec^{-1}$ at L $\sim$ 1.9 R_j. However, the ECD peak current is consistent with an upper limit of 1.4×10^{-7} $cm^{-2}sec^{-1}$ - about a factor of 10 lower flux. The discrepancy in this fission cell rate is attributed to either possible pulse pileup by high energy protons in the detectors or to direct energy loss in the cell detectors by nuclei with Z > 1. I have pointed out this data because of the striking peak flux and also the possibility of substantial energetic, high Z particles in fluxes of the inner Jovian magnetosphere. Our own data from the GSFC experiment on Pioneer has suggested to me that there are probably considerable fluxes of energetic high Z fluxes in the inner magnetosphere. This will be interesting to investigate further, of course.

Data from the University of California at San Diego experiment are plotted in Figure 26 [20]. A wide range of fluxes of electrons are shown as a function of time (or radial distance), as well as the fluxes of protons with energies greater than 80 MeV. I wish to point out two expecially interesting phenomena. Just outside the orbit of Io, the data show that the flux of electrons of energy E > 0.46 MeV jumped by more than a factor of 10. This is inferred to be evidence of particle acceleration near or on the flux tubes associated with Io. The authors point out that from the point of view of decametric radio noise emission, a conservative estimate of the power in the particles near Io is $\sim 10^{13}$ watts, and that this could easily supply the 10^{8} watts of radio power observed [20].

The second phenomena is detailed in the highest energy data shown to the right of Figure 26. While the fluxes are extremely large and dangerous to the spacecraft instrumentation, what is really interesting are the variations in the data. Particles removal by Amalthea apparently can explain two of the minima, but lacking unknown solid material orbiting Jupiter inside the orbit of Amalthea, it would seem that we need a more complicated magnetic field with high order poles to explain these effects.

6. Conclusions.

In summary, the Pioneer 10 and 11 encounters with the Jovian magnetosphere produced most interesting information, contrasts and new phenomena compared to our own earth's magnetosphere. Pioneer 10 had early produced a picture of the Jovian magnetodisk similar to that shown in Figure 27. The energetic particles seemed to be restricted to a rather thin region in the outer magnetosphere, as shown by the shaded areas. The shape of the magnetopause was felt to be not nearly so blunt as the bow shock. The region to the right side was speculatively drawn in as a mirror image.

The crude drawing in Figure 28 more accurately reflects our knowledge after the Pioneer 11 encounter. The outer magnetosphere extends to very high latitudes, and in fact, higher fluxes were measured on Pioneer 11 in the outer magnetosphere at high latitudes than the peak fluxes in the same region near the equator on Pioneer 10. Clearly the simple magnetodisk model has troubles. Explanations may be forthcoming in terms of azimuthal affects and/or temporal variations.

The magnetic field data are consistent for both encounters over much of the magnetosphere. But in close to the planet the two magnetic field experiments do not agree in detail; and it is clear that the energetic particle data need a field with high order poles in order to explain and organize the data. The plasma analyzer clearly maps the bow shock and magnetopause for us; and after a difficult correction to the data for penetrating radiation effects, a most interesting picture of the Jovian plasmosphere, the ring current and the current sheet inferred from the magnetic field measurements emerges.

We have seen large and sometimes unexplained azimuthal effects in the Jovian magnetosphere. Even though we have the Mariner-Jupiter-Saturn spacecraft now being built for a 1977 launch, their trajectories by Jupiter are not a great deal different from Pioneer 10. So an extensive look at this giant magnetosphere must await the orbiters planned tentatively for the early 1980's - especially to allow our first investigations of the dusk side and the tail region, detailed investigations of the role of the plasma, of waves in the magnetosphere, and of particle acceleration and removal in the vicinity of the moons.

Table 1

List of Experiments

INSTRUMENT	INSTITUTION	PRINCIPAL INVESTIGATOR
Helium vector magnetometer	Jet Propulsion Laboratory (JPL)	E. J. Smith
Flux-gate magnetometer	Goddard Space Flight Center (GSFC)	M. Acuna
Plasma analyzer	Ames Research Center (ARC)	J. H. Wolfe
Charged-particle detector	University of Chicago	J. A. Simpson
Geiger-tube telescope	University of Iowa	J. A. Van Allen
Cosmic-ray telescope	Goddard Space Flight Center (GSFC)	F. B. McDonald
Trapped radiation detector	University of California, San Diego (UCSD)	R. W. Fillius

FIGURE CAPTIONS.

Figure 1 - A sketch of the Pioneer 10 Spacecraft [5].

Figure 2 - The Pioneer 10 and Pioneer 11 trajectories referenced to Jupiter and projected into a plane parallel to the ecliptic plane is shown on the left. On the right the trajectories are referenced to Jupiter as seen from earth [5].

Figure 3 - Preliminary half-hour averages of proton bulk speed, number density, and isotropic temperature measured on the Pioneer 11 inbound trajectory [4].

Figure 4 - Pioneer 11 and Pioneer 10 bow shock (circles) and magnetopause crossing (squares) locations [4].

Figure 5 - The proton densities within the energy range 108 eV to 4.80 KeV of the electrostatic analyzer. The magnetic shell parameter L and the pitch angle α of the measurement of directional intensities are given along the top border [13].

Figure 6 - Summary of the major plasma features deep within the Jovian magnetosphere as viewed in a magnetic meridional plane [13].

Figure 7 - Magnitudes of the observed and dipole fields inbound for Pioneer 10 [6].

Figure 8 - Latitudes of observed and dipole fields inbound for Pioneer 10 [6].

Figure 9 - Magnitudes of the observed and dipole fields outbound for Pioneer 10 [6].

the tilt direction of the internal dipole field [12].

Figure 20 - Projection of the trajectories of Pioneer 10 and Pioneer 11 on a magnetic meridian plane of Jupiter based upon the D_2 model [6, 19].

Figure 21 - Inbound and outbound counting rates for detector C (E_e > 21 MeV) of Pioneer 10 as a function of L for the D_2 model [6] is shown on the left, while the right panel shows the same data plotted against a different model and a simple L dependence for M [10].

Figure 22 - Iso-counting rate contours for energetic electron detector C (E_e > 21 MeV) [10].

Figure 23 - Flux profiles of 1.2- to 2.15-MeV and 14.8- to 21.2-MeV protons measured by Pioneer 11 [19].

Figure 24 - Count rate and angular data for the 1.2-, to 2.1-MeV protons are shown for Pioneer 11 plotted against the D_2 model of Smith et al. [6]. The projection of the magnetic field vector on the sector plane is shown.

Figure 25 - The intensity proviles of $\geq$3 MeV electrons, high-energy nuclei, and $\sim$1 MeV protons measured by Pioneer 11 as a function of the magnetic shell parameter L [17].

Figure 26 - Integral fluxes of protons and electrons of kinetic energies greater than the values indicated [20].

Figure 27 - A sketch of the magnetosphere or magnetodisk of Jupiter which resulted from early analysis of the Pioneer 10 results.

Figure 28 - A crude sketch representing our present ideas of the Jovian magnetosphere. The field lines in the tail region are pure speculation, of course.

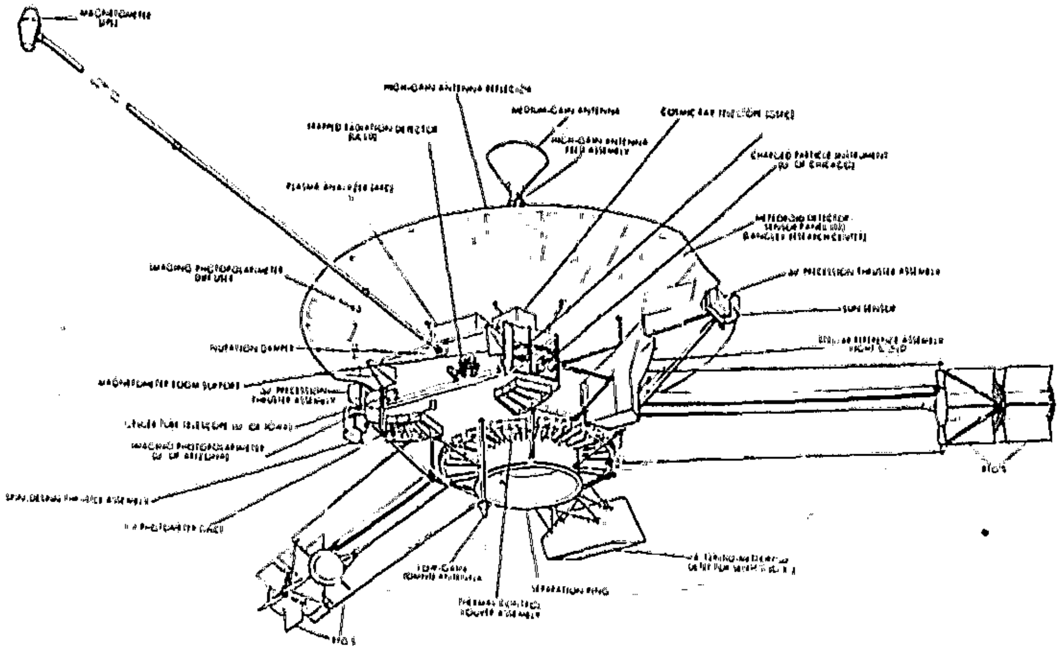

FIG. 1

ORIGINAL PAGE IS
OF POOR QUALITY

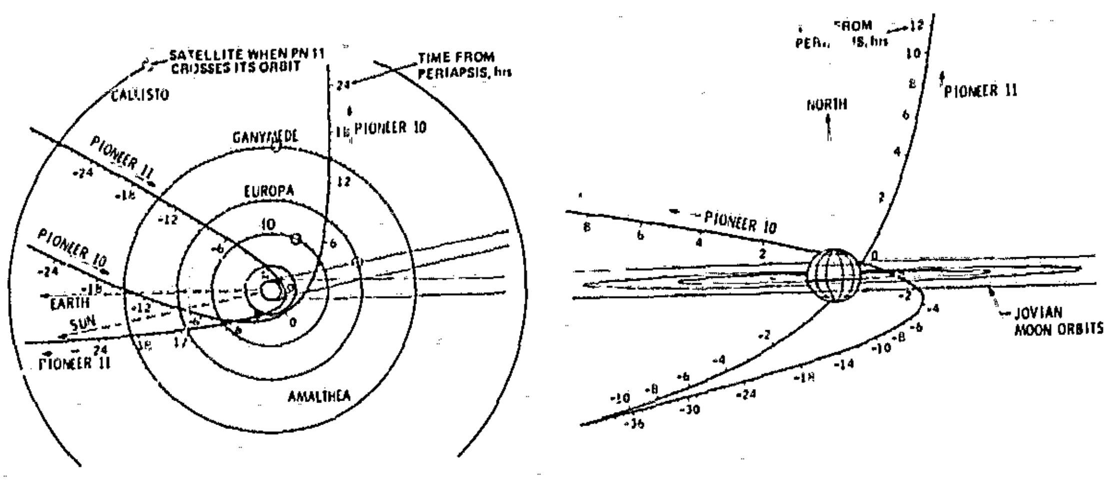

FIG. 2

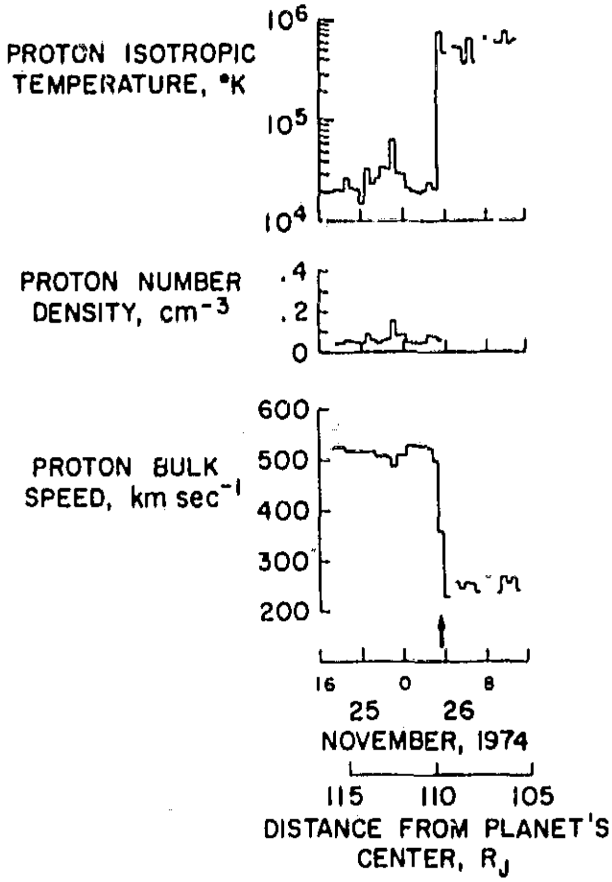
PROTON ISOTROPIC TEMPERATURE, °K
10^6
10^5
10^4
PROTON NUMBER DENSITY, cm^{-3}
.4
.2
0
PROTON BULK SPEED, km sec^{-1}
600
500
400
300
200
16
0
8
25
26
NOVEMBER, 1974
115
110
105
DISTANCE FROM PLANET'S CENTER, R_J

FIG. 3

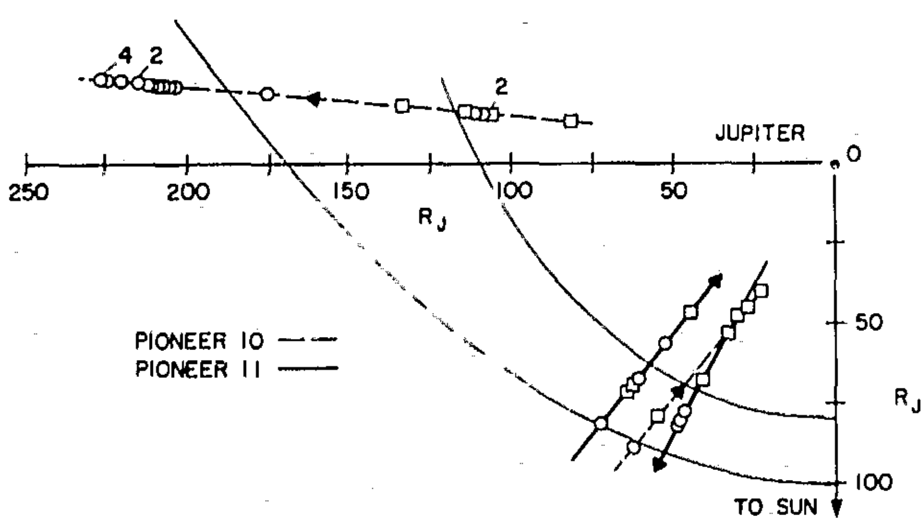
4
2
2
JUPITER
0
250
200
150
100
50
R_J
50
R_J
100
TO SUN
PIONEER 10
PIONEER 11

FIG. 4

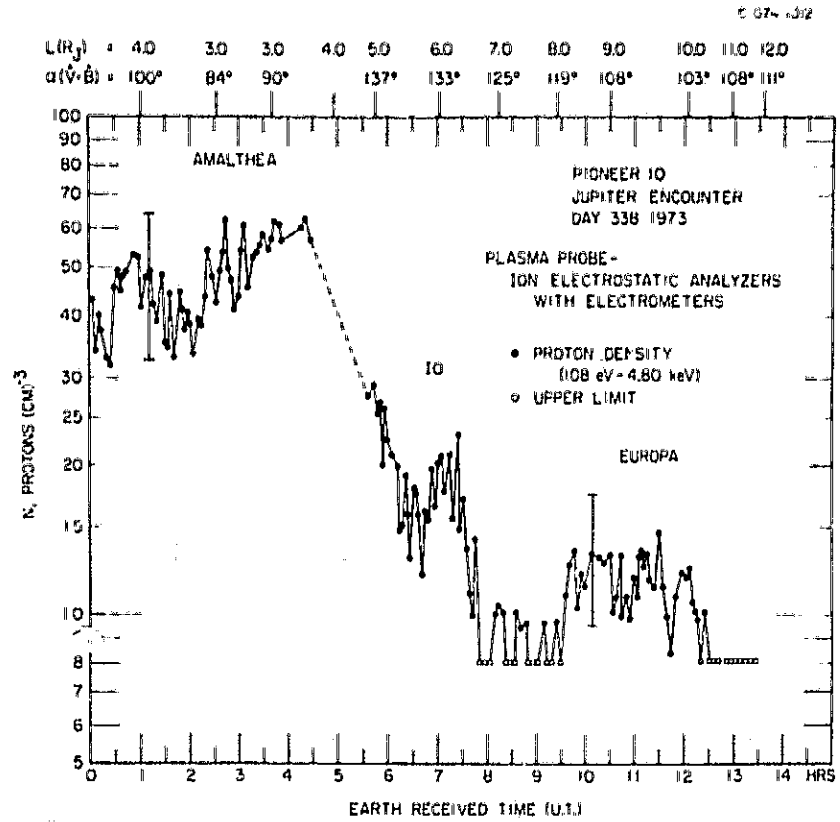

FIG. 5

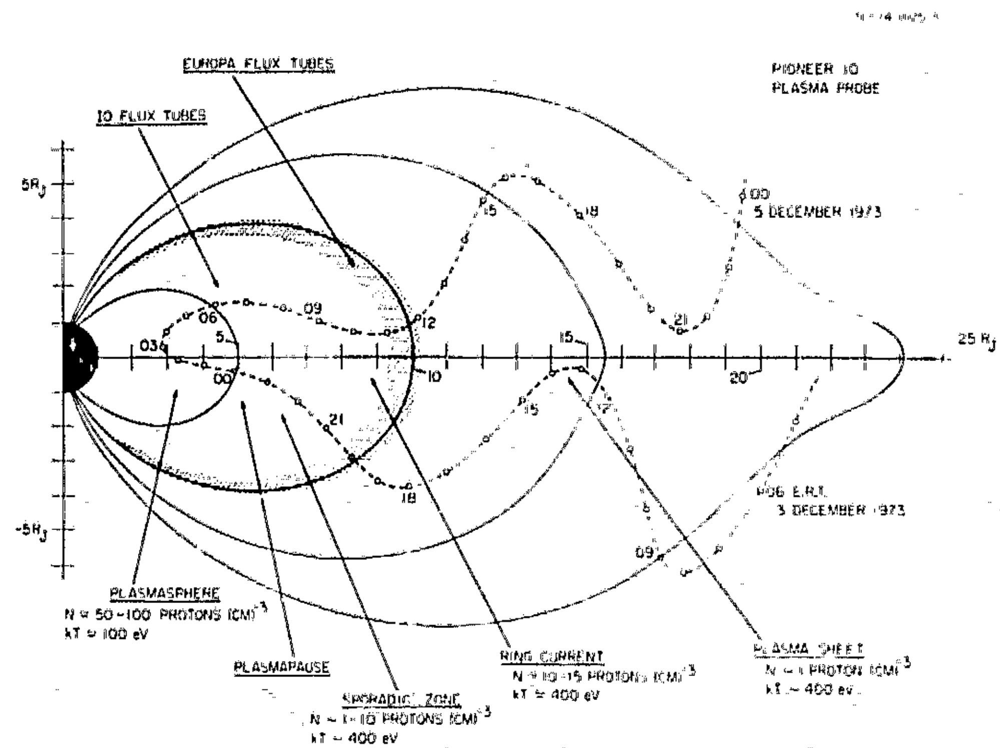

PLASMAS WITHIN THE JOVIAN MAGNETOSPHERE

FIG. 6

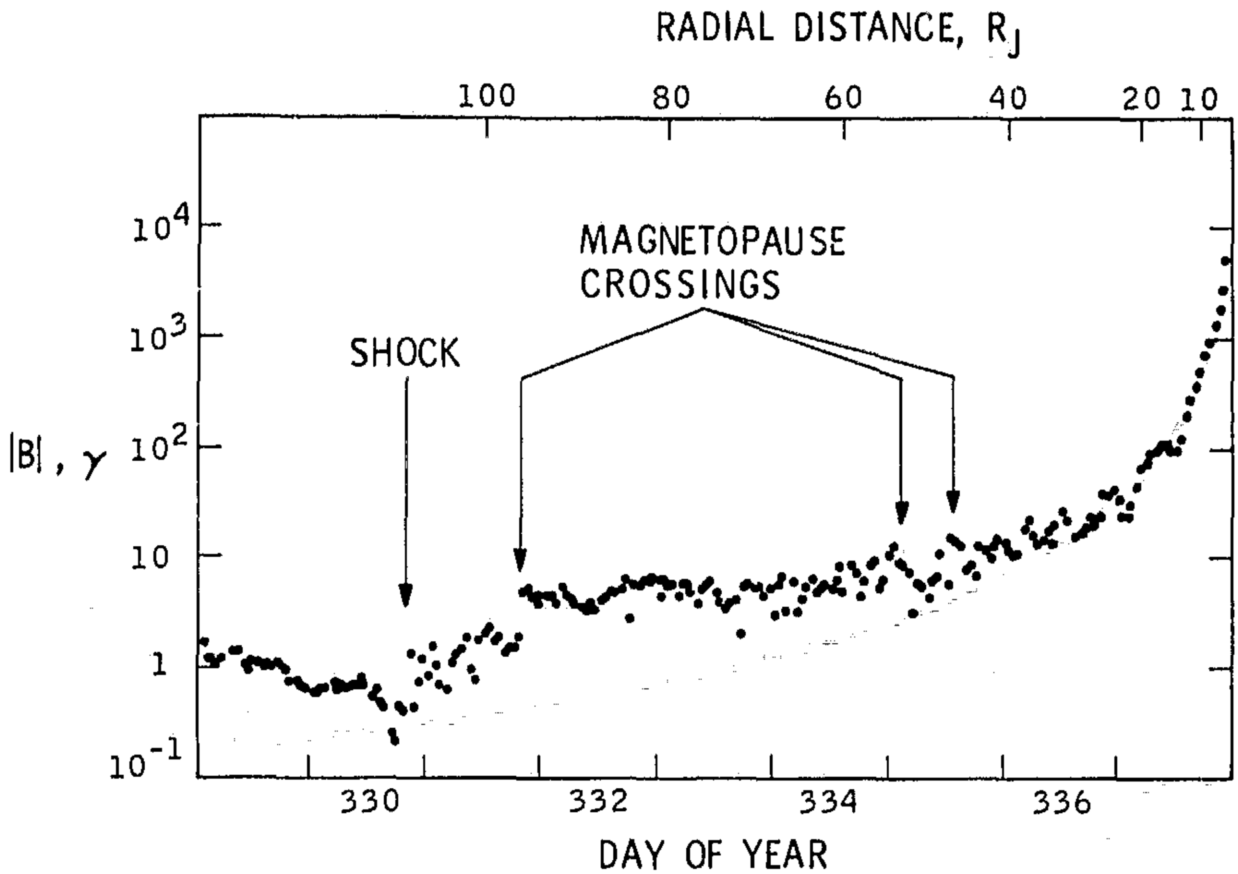
RADIAL DISTANCE, R_J
100
80
60
40
20 10
10^4
10^3
10^2
10
1
10^{-1}
|B|, γ
MAGNETOPAUSE
CROSSINGS
SHOCK
330
332
334
336
DAY OF YEAR

FIG. 7

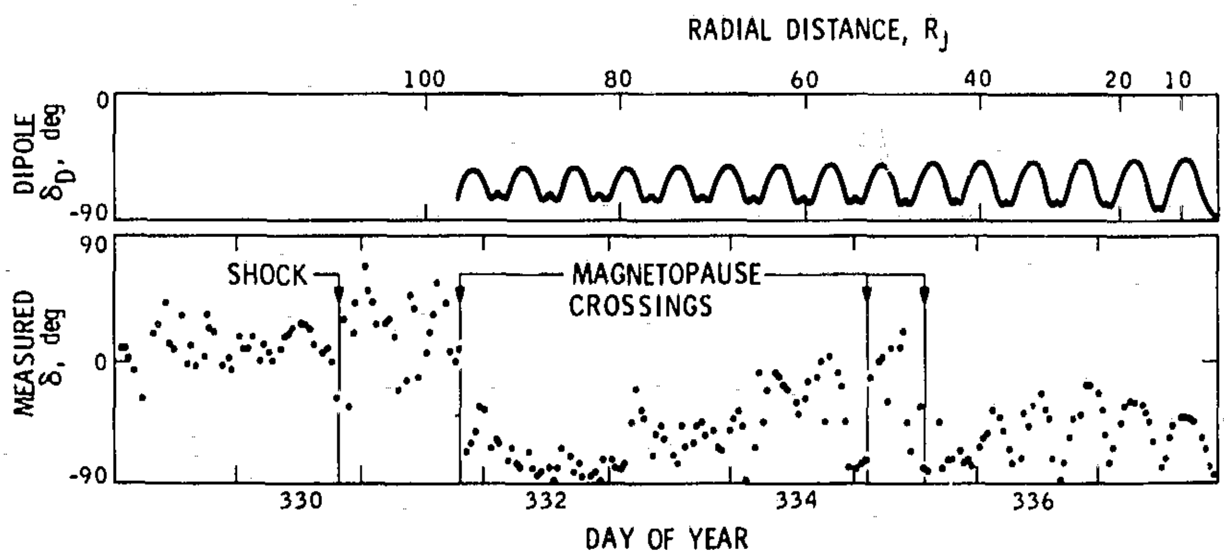
RADIAL DISTANCE, R_J
100
80
60
40
20
10
DIPOLE
δ_D, deg
0
-90
90
0
-90
MEASURED
δ, deg
SHOCK
MAGNETOPAUSE
CROSSINGS
330
332
334
336
DAY OF YEAR

FIG. 8

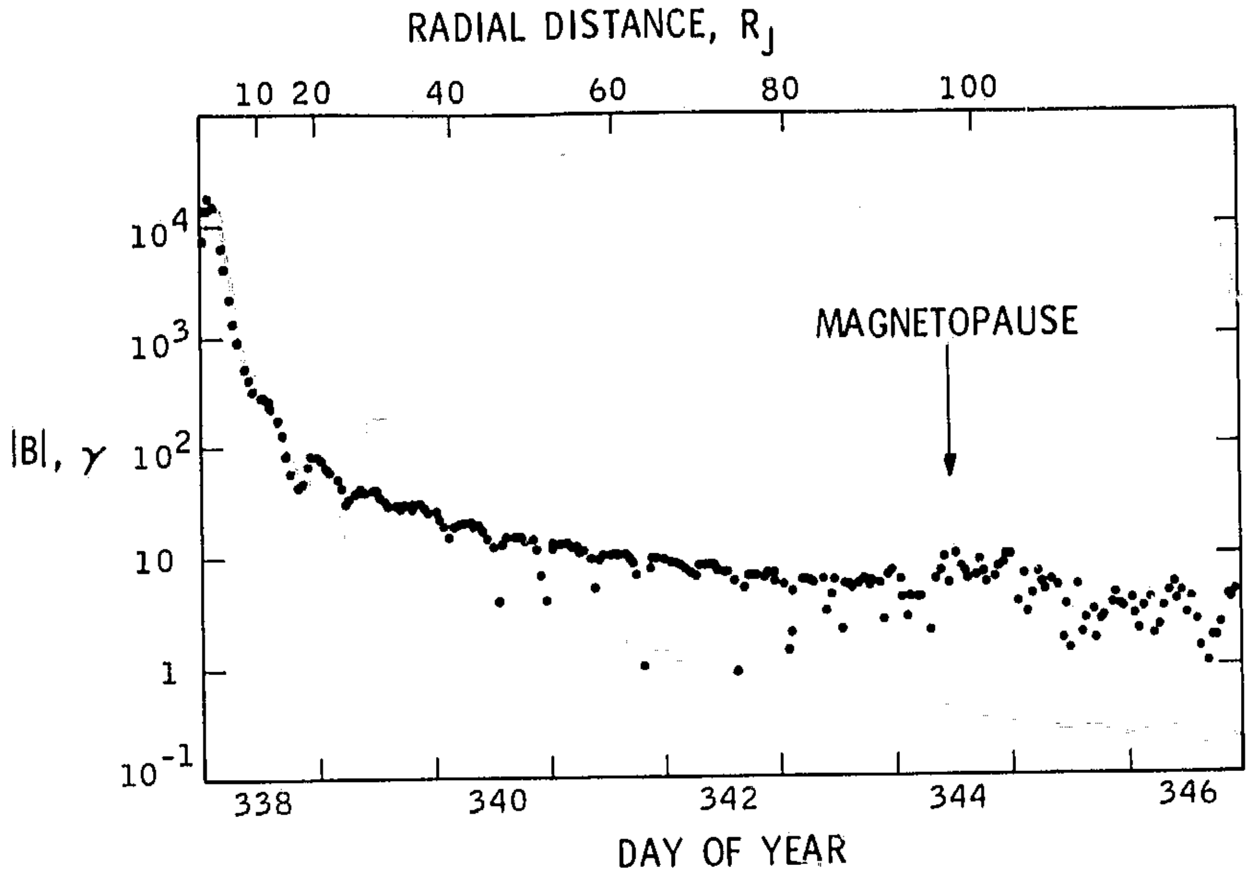
RADIAL DISTANCE, R_J
10 20 40 60 80 100
10^4
10^3
10^2
10
1
10^{-1}
|B|, γ
MAGNETOPAUSE
338 340 342 344 346
DAY OF YEAR

FIG. 9

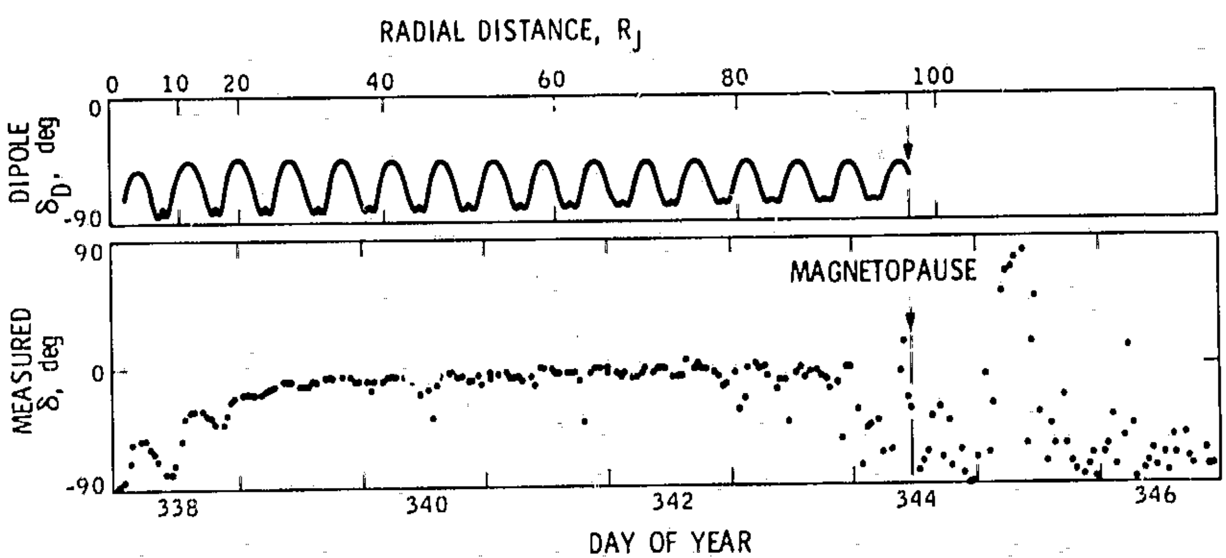
RADIAL DISTANCE, R_J
0 10 20 40 60 80 100
DIPOLE δ_D, deg
0
-90
MEASURED δ, deg
90
0
-90
MAGNETOPAUSE
338 340 342 344 346
DAY OF YEAR

FIG. 10

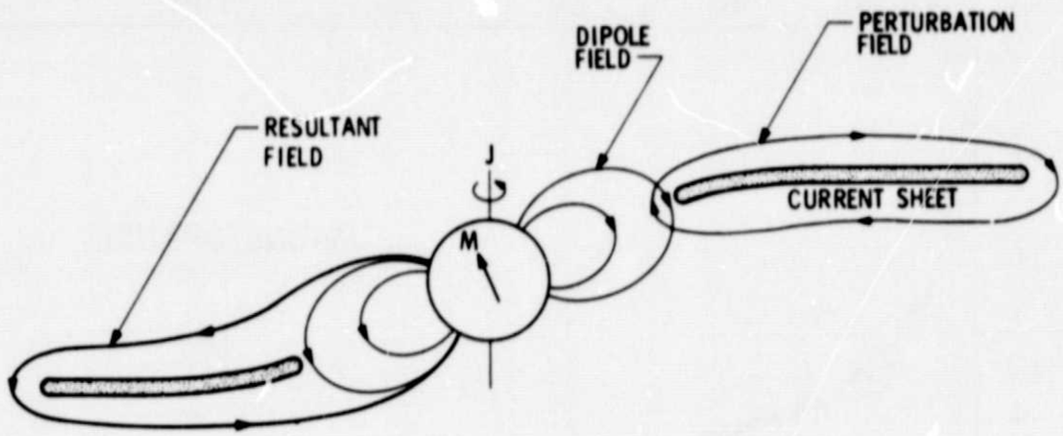
PERTURBATION FIELD
DIPOLE FIELD
RESULTANT FIELD
J
M
CURRENT SHEET

FIG. 11

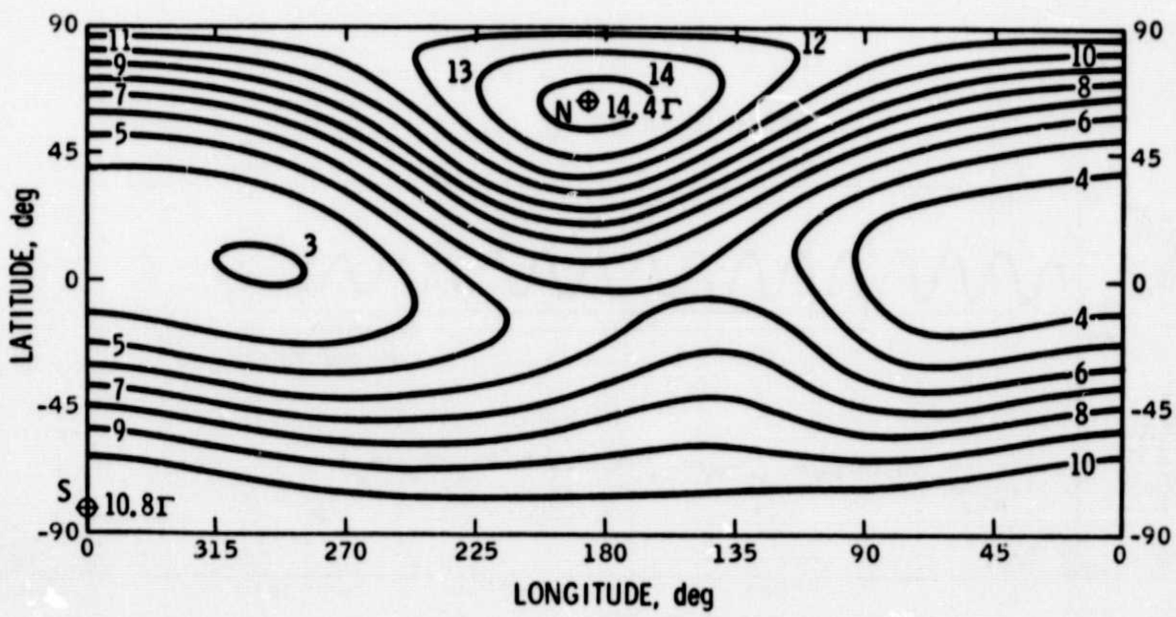
90
45
0
-45
-90
LATITUDE, deg
0
315
270
225
180
135
90
45
0
LONGITUDE, deg
11
9
7
5
12
13
14
N
14.4Γ
10
8
6
4
3
5
7
9
4
6
8
10
S
10.8Γ

FIG. 12

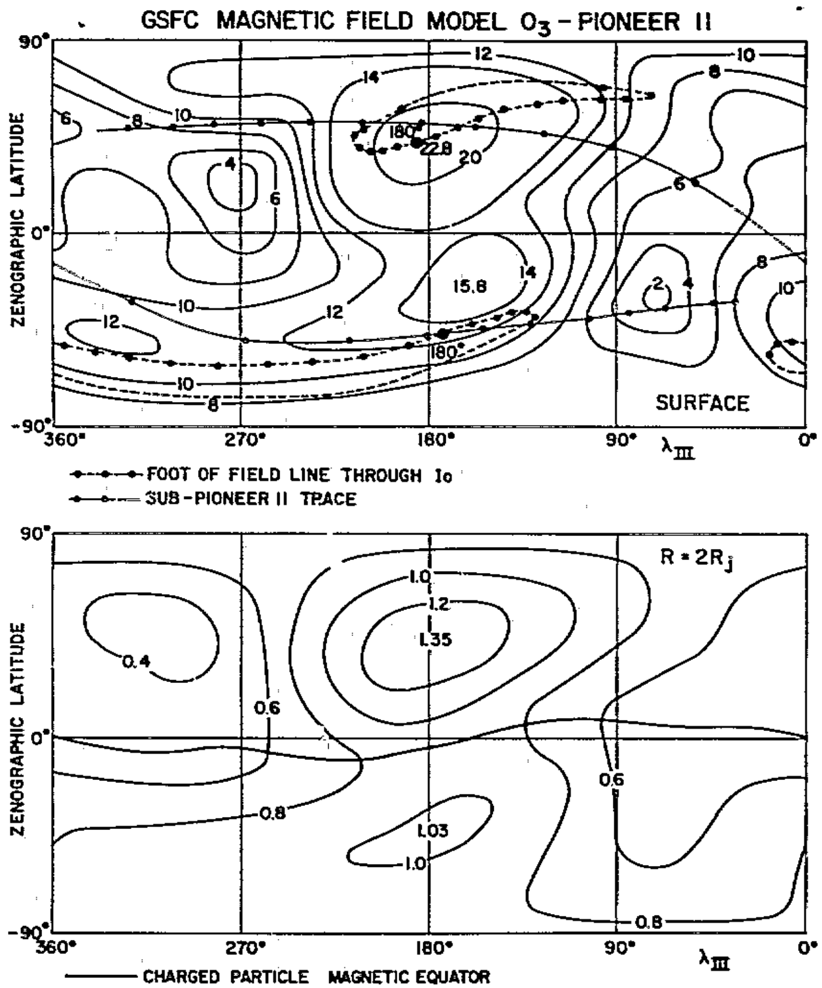
GSFC MAGNETIC FIELD MODEL O3 - PIONEER II
ZENOGRAPHIC LATITUDE
SURFACE
λIII
FOOT OF FIELD LINE THROUGH Io
SUB-PIONEER II TRACE
R = 2Rj
CHARGED PARTICLE MAGNETIC EQUATOR

FIG. 13

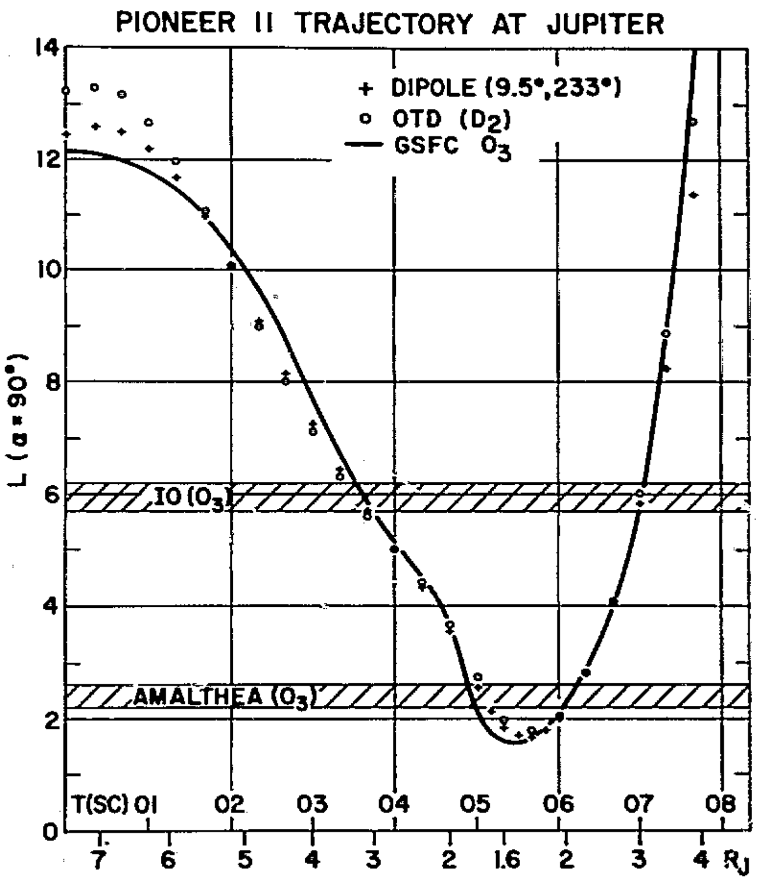
PIONEER II TRAJECTORY AT JUPITER
+ DIPOLE (9.5°,233°)
o OTD (D2)
GSFC O3
L (α = 90°)
IO (O3)
AMALTHEA (O3)
T(SC) 01
RJ

FIG. 14

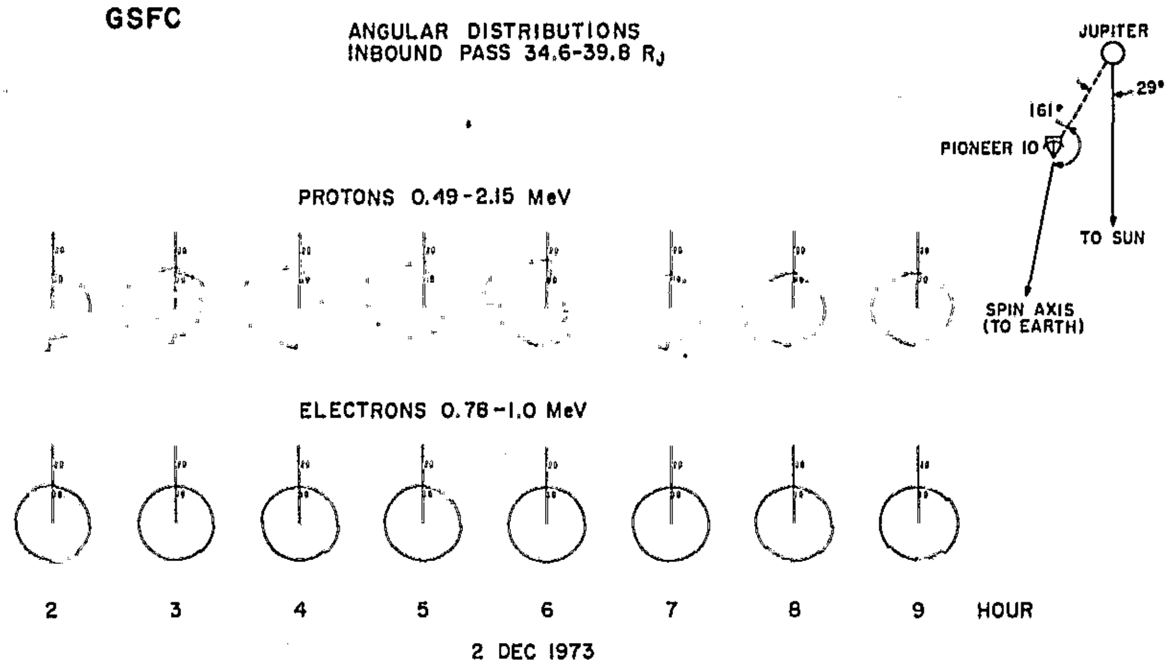

FIG. 17

ORIGINAL PAGE IS
OF POOR QUALITY

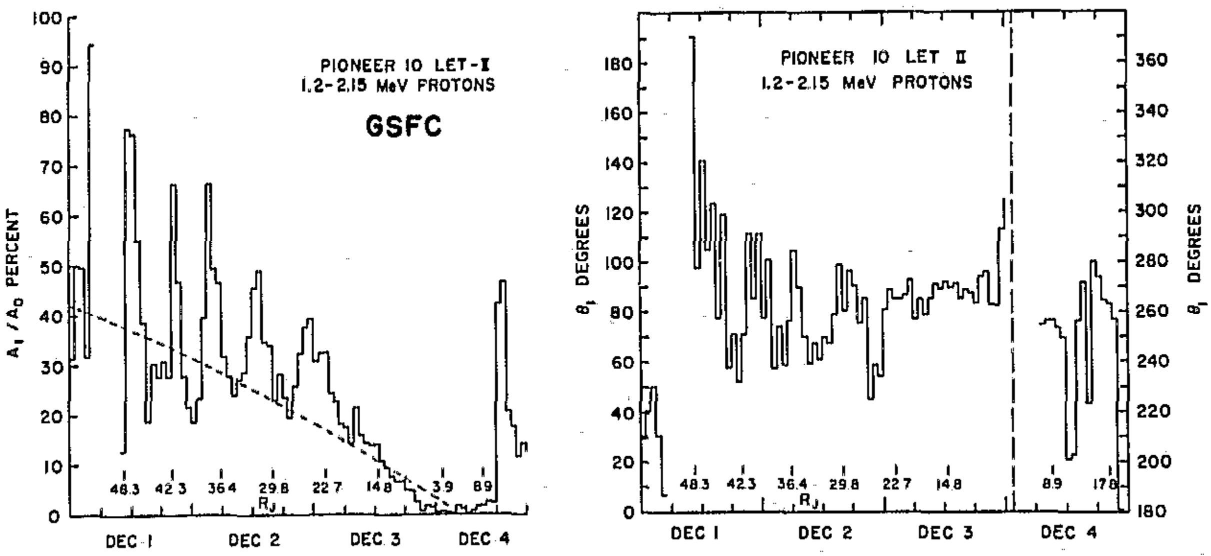

FIG. 18

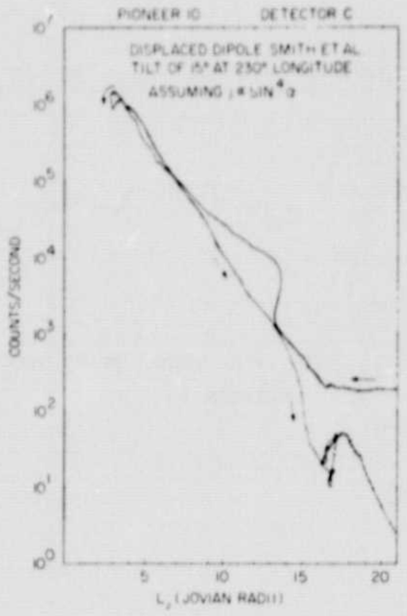
PIONEER 10
DETECTOR C
DISPLACED DIPOLE SMITH ET AL
TILT OF 15° AT 230° LONGITUDE
COUNTS/SECOND
L (JOVIAN RADII)
CENTERED DIPOLE
TILT OF 9.5° AT 230° LONGITUDE
DATA CORRECTED TO EQUATORIAL

FIG. 21

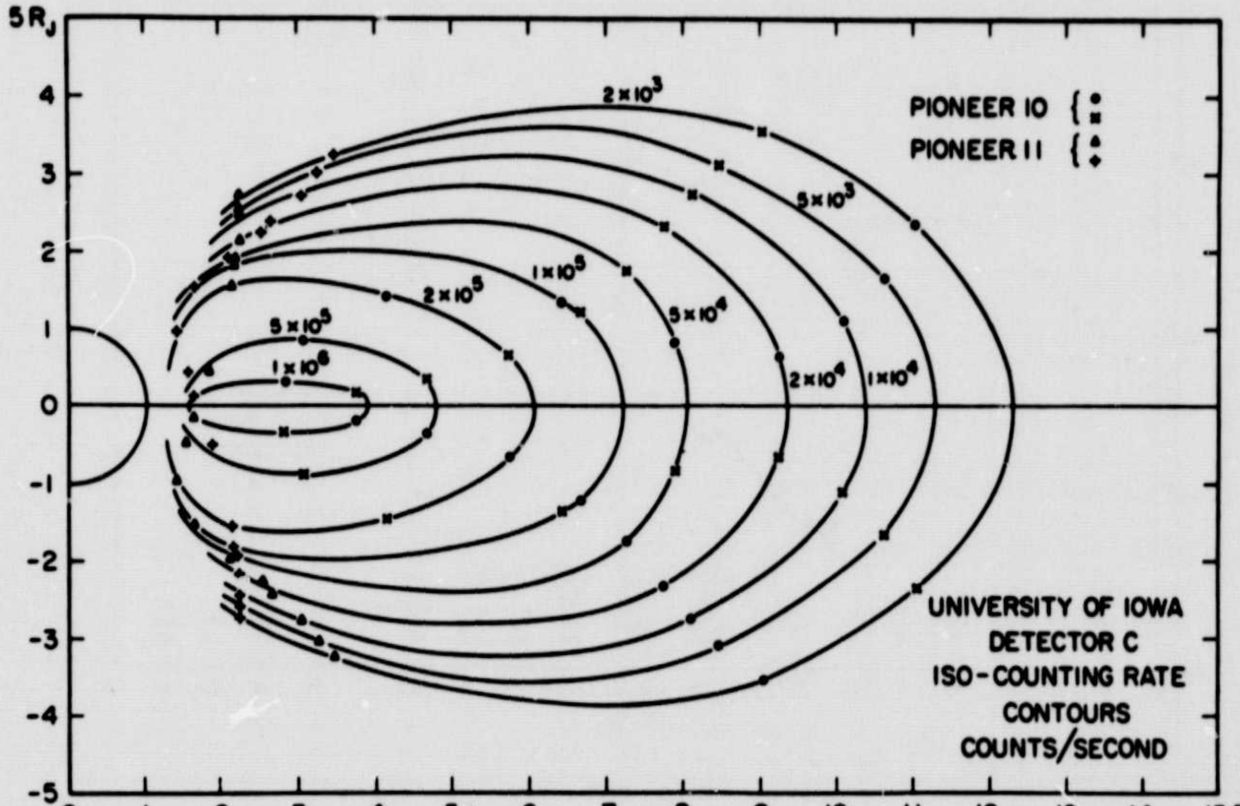
PIONEER 10
PIONEER 11
UNIVERSITY OF IOWA
DETECTOR C
ISO-COUNTING RATE
CONTOURS
COUNTS/SECOND

FIG. 22

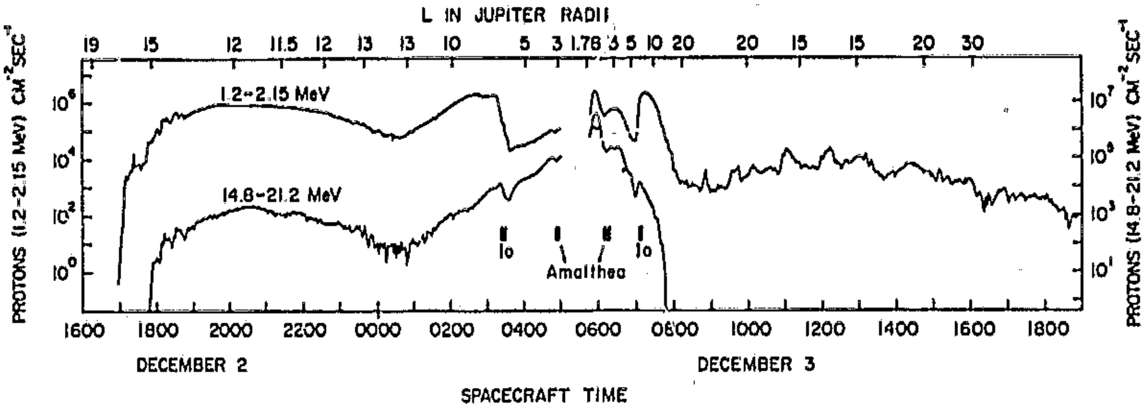
L IN JUPITER RADII
19 15 12 11.5 12 13 13 10 5 3 1.78 3 5 10 20 20 15 15 20 30
1.2-2.15 MeV
14.8-21.2 MeV
Io
Amalthea
Io
PROTONS (1.2-2.15 MeV) CM⁻²SEC⁻¹
PROTONS (14.8-21.2 MeV) CM⁻²SEC⁻¹
1600 1800 2000 2200 0000 0200 0400 0600 0800 1000 1200 1400 1600 1800
DECEMBER 2
DECEMBER 3
SPACECRAFT TIME

FIG. 23

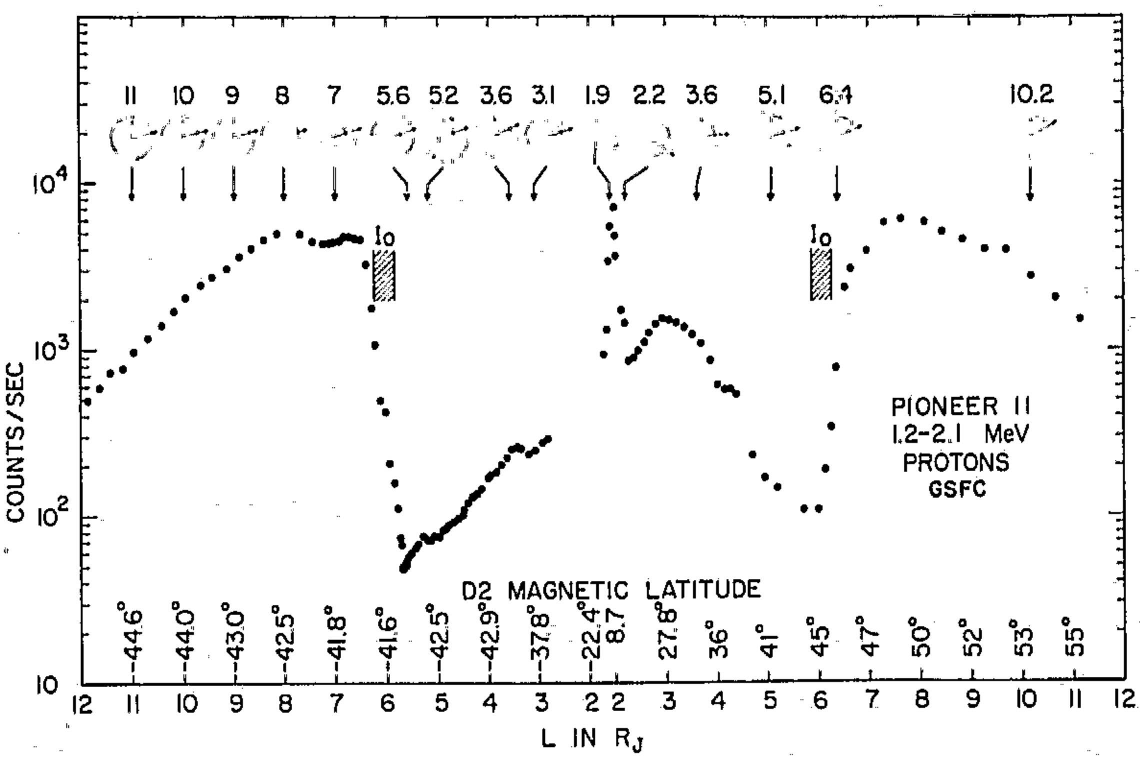
11 10 9 8 7 5.6 5.2 3.6 3.1 1.9 2.2 3.6 5.1 6.4 10.2
Io
Io
COUNTS/SEC
PIONEER 11
1.2-2.1 MeV
PROTONS
GSFC
D2 MAGNETIC LATITUDE
-44.6° -44.0° -43.0° -42.5° -41.8° -41.6° -42.5° -42.9° -37.8° -22.4° 8.7° 27.8° 36° 41° 45° 47° 50° 52° 53° 55°
12 11 10 9 8 7 6 5 4 3 2 2 3 4 5 6 7 8 9 10 11 12
L IN R_J

FIG. 24

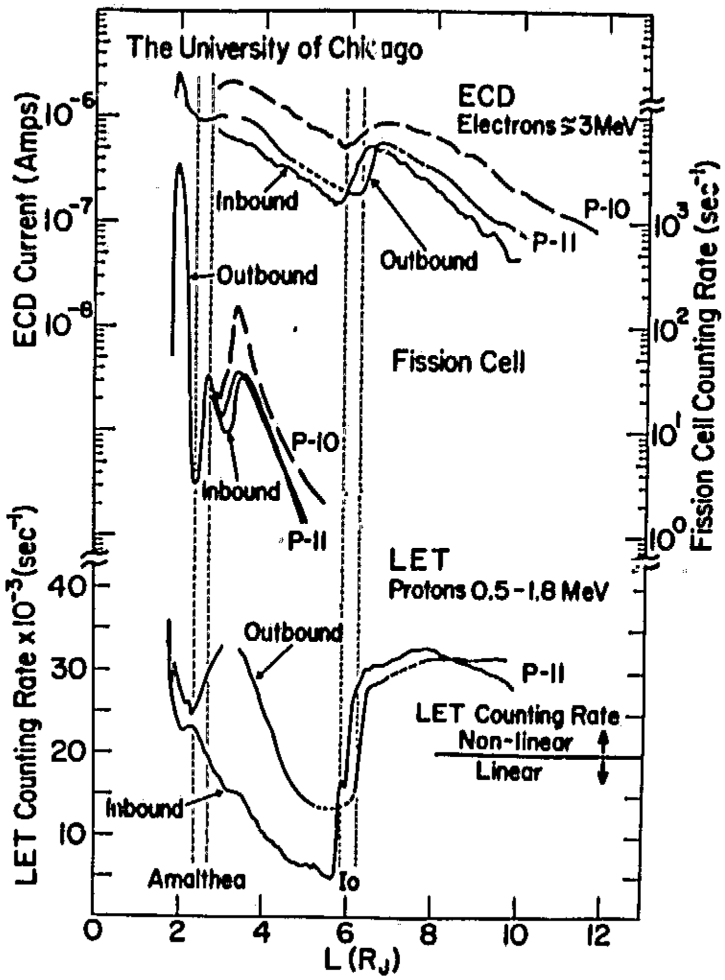
The University of Chicago
ECD
Electrons ≳3MeV
ECD Current (Amps)
10^{-6}
10^{-7}
10^{-8}
Inbound
Outbound
P-10
P-II
Fission Cell
Fission Cell Counting Rate (sec^{-1})
10^3
10^2
10^1
10^0
LET
Protons 0.5-1.8 MeV
LET Counting Rate x10^{-3}(sec^{-1})
40
30
20
10
LET Counting Rate
Non-linear
Linear
Amalthea
Io
0
2
4
6
8
10
12
L(R_J)

FIG. 25

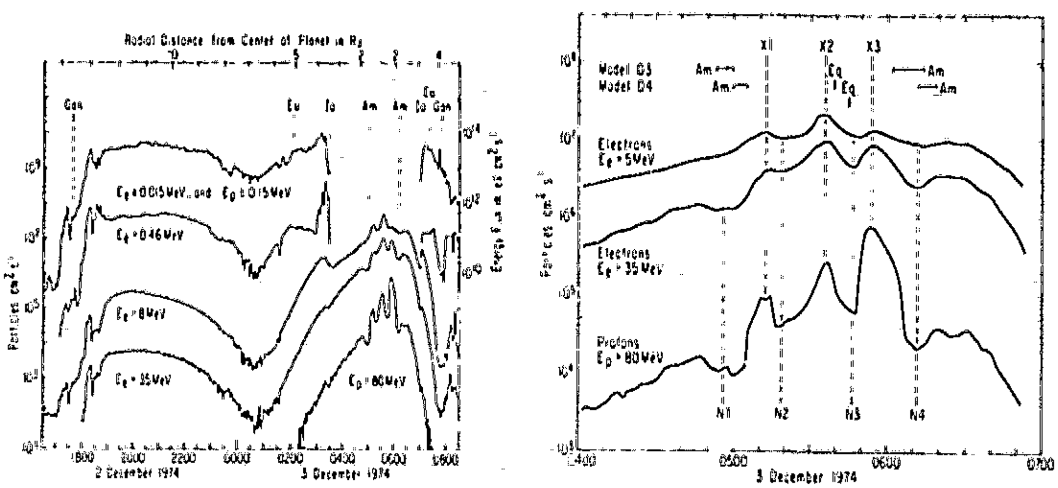
X1
X2
X3
N1
N2
N3
N4
Electrons
Protons
3 December 1974
2 December 1974
0700

FIG. 26

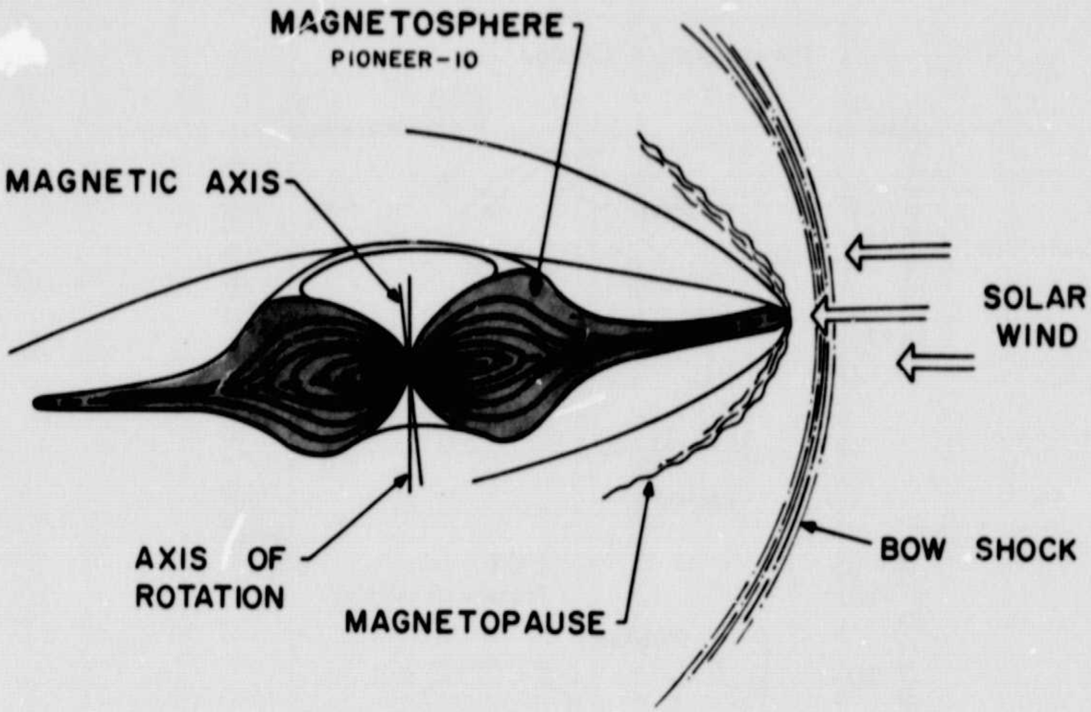
MAGNETOSPHERE
PIONEER-10
MAGNETIC AXIS
SOLAR
WIND
AXIS OF
ROTATION
BOW SHOCK
MAGNETOPAUSE

FIG. 27

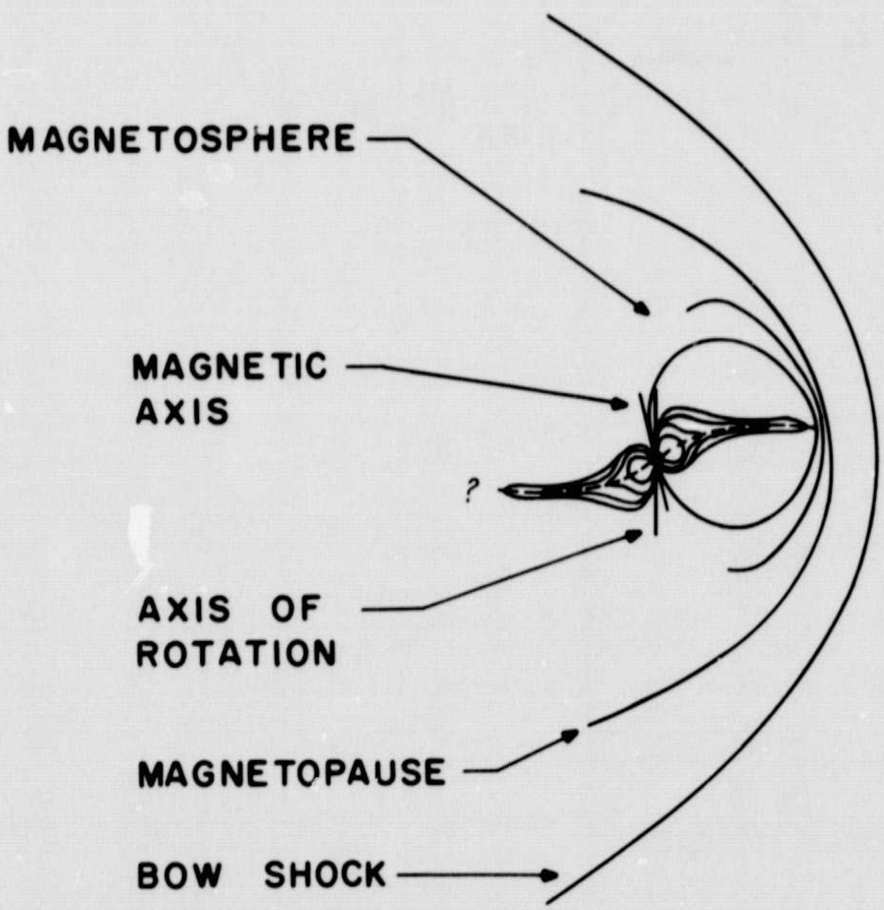
MAGNETOSPHERE
MAGNETIC
AXIS
?
AXIS OF
ROTATION
MAGNETOPAUSE
BOW SHOCK

FIG. 28

REFERENCES.

[1] T. D. Carr and S. Gulkis, Ann. Rev. Astron. Astrophys. 7, 577 (1969).

[2] J. W. Warwick, Space Sci. Revs. 6, 841 (1967).

[3] J. H. Wolfe et al., Science 183, 303 (1974).

[4] J. D. Mihalov et al., Science 188, 448 (1975).

[5] C. F. Hall, Science 188, 446 (1975).

[6] E. J. Smith et al., J. Geophys. Res. 79, 3501 (1974).

[7] M. H. Acuna and N. F. Ness, The Complex Magnetic Field of Jupiter, in publication, J. Geophys. Res. (1975).

[8] J. H. Wolfe et al., J. Geophys. Res. 79, 3489 (1974).

[9] J. A. Simpson et al., J. Geophys. Res. 79, 3522 (1974).

[10] J. A. Van Allen et al., J. Geophys. Res. 79, 3559 (1974).

[11] D. E. Stilwell et al., IEEE Trans. Nuc. Sci. 22, 570 (1975).

[12] R. W. Fillius and C. E. McIlwain, J. Geophys. Res. 79, 3589 (1974).

[13] L. A. Frank et al., Observations of Plasmas in the Jovian Magnetosphere, in publication, J. Geophys. Res. (1975).

[14] J. H. Wolfe et al., J. Geophys. Res. 79, 3489 (1974).

[15] E. J. Smith et al., Science 188, 451 (1975).

[16] B. J. Teegarden et al., J. Geophys. Res. 79, 3615 (1974).

[17] J. A. Simpson et al., Science 188, 455 (1975).

[18] J. A. Van Allen et al., Science 188, 459 (1975).

[19] J. H. Trainor et al., Science 188, 462 (1975).

[20] R. W. Fillius and C. E. McIlwain, Science 188, 465 (1975).

[21] J. H. Trainor et al., J. Geophys. Res. 79, 3600 (1974).

[22] G. D. Mead, J. Geophys. Res. 79, 3487 (1974) and G. D. Mead and R. E. Sweeney, Goddard Space Flight Center Doc. No. X-922-74-339 (November 1974).

[23] G. D. Mead and W. N. Hess, J. Geophys. Res. 78, 2793 (1973) and W. N. Hess et al., ibid, 79, 2877 (1974).

[24] M. H. Acuna, personal communication, March 1975.